

# Predicting the Presence of Oral Squamous Cell Carcinoma Using Commonly Dysregulated MicroRNA in Oral Swirls



Tami Yap<sup>1</sup>, Kendrick Koo<sup>2</sup>, Lesley Cheng<sup>3</sup>, Laura J. Vella<sup>4</sup>, Andrew F. Hill<sup>3</sup>, Eric Reynolds<sup>1,5</sup>, Alf Nastri<sup>6</sup>, Nicola Cirillo<sup>1,5</sup>, Christine Seers<sup>1,5</sup>, and Michael McCullough<sup>1,5</sup>

## Abstract

Oral swirls are a noninvasive, rapidly collected source of salivary microRNA (miRNA) potentially useful in the early detection of disease states, particularly oral squamous cell carcinoma (OSCC). The aim of this study was to predict the presence of OSCC using a panel of OSCC-related dysregulated miRNA found in oral swirls, identified jointly in data from formalin-fixed paraffin-embedded (FFPE) and fresh-frozen specimens. Next-generation sequencing (NGS) was used to determine miRNA fold changes in FFPE OSCC specimens relative to histologically normal epithelium. These data were placed with NGS of fresh-frozen tissue data of The Cancer Genome Atlas database to select a panel of commonly dysregulated miRNA. This panel was then analyzed by RT-qPCR in RNA extracted from oral swirls collected from 30 patients with OSCC

and 30 controls. Upregulation of miR-31 and miR-21 and downregulation of miR-99a, let-7c, miR-125b, and miR-100 were found between OSCC and controls in both FFPE and fresh-frozen samples. These miRNAs were studied in a training set of 15 OSCC versus 15 control oral swirls to develop a dysregulation score [AUC, 0.95; 95% confidence interval (CI), 0.88–1.03] and classification tree. A test cohort of 15 OSCC versus 15 control oral swirls yielded a dysregulation score AUC of 0.86 (95% CI, 0.79–1.00) with the classification tree identifying 100% (15/15) of OSCC and 67% (10/15) of controls. This study debuts the use of OSCC-associated miRNA, commonly dysregulated in both FFPE and frozen specimens, in oral swirls to indicate the presence of OSCC with high accuracy. *Cancer Prev Res*; 11(8); 491–502. ©2018 AACR.

## Introduction

It is well established that oral carcinogenesis results from accumulation of genetic alterations in squamous mucosa, which leads to malignant transformation of normal oral epithelium. Oral squamous cell carcinoma (OSCC) may be preceded by morphologic alterations of the oral mucosa; however, the clinical trajectory of these remains stubbornly unpredictable. Precursor mucosal changes, grouped together as oral potentially malignant disorders (OPMD), vary from small well-defined white or red mucosal patches to widespread and extensive changes of the oral mucosa.

Approximately 2.6% of the population is affected by OPMD, such as oral leukoplakia and oral lichen planus (OLP), and it is estimated that 1% to 3% of individuals with OPMD will go on to develop OSCC (1, 2). Diagnosis of OSCC and OPMD is currently made by clinical evaluation and scalpel biopsy of a discernable lesion. Sampling error and intra- and interobserver reliability remain an issue with histopathologic assessment of specimens having a false-negative rate of up to 10% (3). Further, malignant change can develop in an area that does not exhibit clinical or histopathologic abnormality; thus, ways to assess the entire oral mucosal field are desired.

When diagnosed at a late stage, treatment of OSCC is highly debilitating, and the disease is often fatal. Early stage OSCC, however, has a favorable prognosis and requires less aggressive treatment. Unfortunately, OSCC often goes unnoticed or can be misdiagnosed by primary care practitioners (4). Almost half of patients experience diagnostic delay, and over 50% of patients present with advanced stage of disease (5). Hence, early detection is key. Identification of OSCC at a molecular level preceding clinical and histopathologic evident change will transform diagnosis into prognosis. Further, risk stratification is desired not

<sup>1</sup>Melbourne Dental School, University of Melbourne, Victoria, Australia. <sup>2</sup>Department of Surgery, Royal Melbourne Hospital, Victoria, Australia. <sup>3</sup>Department of Biochemistry and Genetics, La Trobe Institute for Molecular Science, La Trobe University, Victoria, Australia. <sup>4</sup>The Florey Institute of Neuroscience and Mental Health, Parkville, Victoria, Australia. <sup>5</sup>Oral Health Cooperative Research Centre, Melbourne, Victoria, Australia. <sup>6</sup>Department of Oral and Maxillofacial Surgery, Royal Melbourne Hospital, Victoria, Australia.

**Corresponding Author:** Tami Yap, University of Melbourne, Melbourne, VIC 3124, Australia. Phone: +61 3 93411120; E-mail: tsyap@unimelb.edu.au

doi: 10.1158/1940-6207.CAPR-17-0409

©2018 American Association for Cancer Research.

only in individuals who present with OPMD but, also, for the general population, particularly those exposed to risk factors for OSCC.

An ideal diagnostic test would be quick and easily collected at point of care. An appropriate sampling method is an oral swirl, which comprises 10 mL of sterile deionized water, swirled like a mouthwash for 50 seconds before expectoration into a tube (6). The resulting sample includes the deionized water, saliva, and other oral contents. Specialized devices and training are not required for administration of oral swirls. We have recently shown that oral swirls can be used as a source of microRNAs (miRNA), which are likely to be contained in and protected by extracellular vesicles (6). Changes in miRNA expression have been associated with almost all human malignancies and may be considered an indicator of activity within the cells. Thus, altered miRNA expression is a candidate marker of early malignant change in the absence of clinically visible mucosal change. Analysis of miRNAs isolated from oral swirls could be used to identify malignant changes within the oral cavity.

Analytic techniques used to analyze RNA and DNA, including microarrays, PCR, and next-generation sequencing (NGS), are also applicable to miRNA. NGS has successfully identified miRNA expression profiles in patients with OSCC, whereas microarrays and PCR have been used successfully to investigate biofluids including serum, plasma, and salivary miRNA (7, 8). Comparison of prospectively collected clinical samples with archived formalin-fixed paraffin-embedded (FFPE) and frozen specimens is required to bridge application of retrospective genomic studies. MiRNA has been shown to be fit for this purpose, with expression profiles consistent between fresh-frozen and FFPE in pairwise analyses in other malignant tissues (9). MiRNAs discovered to have shared dysregulation in both frozen resection specimens and FFPE diagnostic biopsy may also be detectable and dysregulated in oral swirls.

We aimed to identify miRNA dysregulated in OSCC using NGS of RNA isolated from FFPE tissue from diagnostic biopsy collected by the Royal Dental Hospital (RDH). These dysregulated miRNAs were then compared with alterations identified in fresh-frozen tissues by The Cancer Genome Atlas (TCGA) database. Finally, alterations of commonly identified dysregulated miRNAs in oral swirl samples from patients with OSCC were elucidated.

## Materials and Methods

This study was approved by the Human Research Ethics Committee of the University of Melbourne (Ethics ID: 050900X) and Melbourne Health (Ethics ID: 2014.111).

### The RDH-NGS dataset

FFPE material from the incisional biopsies of 12 patients attending the Oral Medicine Department of the Royal

Dental Hospital of Melbourne was collected. These included 3 histologically normal epithelium (HNE), 3 OSCC, 3 specimens of OLP, and 3 specimens with epithelial dysplasia.

RNA from 4 × 20 μm FFPE sections was extracted using the RecoverAll Isolation Kit and concentrated to 15 μL using a rotational vacuum concentrator. RNA quality was assessed using an Agilent 2100 Bioanalyzer using the small RNA assay and RNA Nano 6000 assay. Small RNA libraries were constructed using 100 ng of the RNA using the Ion Total RNA-Seq Kit V2 (Life Technologies) and ligated to adapters containing a unique index barcode (Ion Xpress RNA-Seq Barcode 1–16 Kit, Life Technologies). The yield and size distribution of the small RNA libraries were assessed using the Agilent 2100 Bioanalyzer instrument with the DNA 1000 chip (Agilent Technologies). Equally pooled libraries were prepared for templating on the Ion Chef system (Life Technologies) and sequenced on the Ion Torrent S5 using Ion 540 chips (Life Technologies) and 200 bp chemistry (Life Technologies). Preprocessing of reads and removal of adapters and barcodes were performed using the Torrent Suite (v.5.0.2).

The raw NGS sequence data were aligned to hg19 using the TMAP aligner, and aligned reads were mapped to miRBase 21. The EdgeR library was used for normalization of count data (10). MiRNAs with <30 normalized reads across all samples were discarded.

### TCGA-NGS dataset

TCGA data for oral cavity squamous cell carcinoma samples were retrieved, with a census date set at May 2015. This dataset included 292 oral cavity OSCC and 30 normal samples. The EdgeR and limma libraries were used for identification of differentially expressed miRNAs (10).

### Oral swirl-PCR analysis

Oral swirl samples were collected from 30 patients with OSCC (OSCC-OS; mean age, 64.8; 17 males and 13 females) and 30 controls (C-OS; mean age, 58.0; 16 males and 14 females). Recorded habits included smoking (OSCC-OS: current, 9; past, 5; never, 16; C-OS: current, 14; never, 16) and daily alcohol consumption (OSCC-OS: yes, 10; no, 20; C-OS: yes, 5; no, 25). The OSCC-OS cohort included individuals with both early and advanced disease: T classification (T1–16, T2–4, T3–1, T4a–9) and stage (I–14, II–3, III–3, IV–10). The patients were asked to swirl 10 mL of sterile deionized water for 50 to 60 seconds and expectorate into a sterile container. The oral swirls were centrifuged at 4000 × g for 4 minutes at 4°C to pellet the cells which were discarded. The resultant cell-free swirl (OS) was stored at –20°C. Preparation to enrich for contained extracellular vesicles was undertaken as previously described (6). Briefly, after defrosting the OS samples (5 × 1 mL aliquots) on ice each aliquot added to 1 mL of 40% w/v polyethylene glycol (PEG) 6000 (Sigma-Aldrich)

and incubated overnight at 4°C in a 2.2 mL microcentrifuge tube. The 5 aliquots per sample were then centrifuged at 10,000 × g for 30 minutes before the supernatant was removed leaving approximately 100 µL of precipitant in each. The precipitants were vortexed, pooled, centrifuged at 10,000 × g for 5 minutes, and 400 µL of the supernatant removed giving 100 µL of precipitant from the original 5 × 1 mL aliquots. A pellet was not always visible.

RNA was extracted from the final OS precipitant using the mirVana microRNA isolation Kit (Life Technologies) beginning with 300 µL of lysis buffer. Yield was measured using a NanoDrop spectrophotometer (NanoDrop1000; NanoDrop Technologies). Samples were concentrated to 20 µL using centrifugation under vacuum, and RNA yield was measured using a Nanodrop spectrophotometer. Each reverse transcription reaction had 80 ng of RNA. A custom reverse transcription (RT) primer pool was designed for use with the EPIK microRNA Select Assay Kit (Bioline, Alexandria, Australia) (11), and qPCR was performed in duplicate on an Eco, Illumina PCR machine. Human heart RNA (Life Technologies) was used as a positive RNA control for RT reactions. The threshold cycle ( $C_t$ ) autothreshold was determined algorithmically within the Eco software using a modified method of Liu and Saint (12). A geometric averaging normalization strategy was used (13). Statistical analyses were performed using GraphPad Prism 7.03; quantified miRNA were assessed using unpaired *t* tests and AUC of the receiver operator characteristic.

## Results

### Discovering a commonly dysregulated miRNA signature in both FFPE and frozen specimens

**NGS of miRNA from FFPE biopsy samples (RDH-NGS).** RNA obtained from 12 FFPE biopsies with diagnoses of OSCC, HNE, OLP, or dysplasia was successfully sequenced by small RNA-seq, with a mean read depth of 3.5 million reads (range, 1.9–5.6 million) and a mean of 84% of reads mapping to miRBase (range, 77%–87%). Of the 2,794 human miRNAs in miRBase, significant numbers of alignments (>30 reads total) were found for 348 miRNA species (12.5%). Log-transformed read counts were visualized on a dendrogram of hierarchical clustering (Fig. 1). This showed OSCC and HNE samples on opposite ends of the spectrum with OLP and dysplasia samples alternating in between.

### Identifying common dysregulation in RDH-NGS and TCGA-NGS datasets

The miRNA abundance distributions of both the RDH-NGS and TCGA-NGS followed a bimodal curve with majority of miRNA species displaying normalized reads counts lower than the geometric median read count of each dataset. There were 236 miRNAs in common between the two datasets obtained from RDH and TCGA. The TCGA-NGS and RDH-NGS read count data were log transformed, and the fold change of each miRNA between

OSCC and controls was determined (Fig. 2A). MiRNAs which were dysregulated by less than  $\pm 1 \log_2$  fold changes in both datasets or had conflicting up- or downregulation between the two datasets were eliminated, leaving 29 miRNAs showing dysregulation in the same direction (Fig. 2B). Hierarchical clustering of these selected miRNA in the TCGA-NGS data yielded a sensitivity of 97.9% and specificity 96.7% to distinguish OSCC from HNE (Fig. 3).

Taken together, these data showed that many miRNAs could be quantified using NGS of FFPE biopsy samples, but only limited candidate miRNAs showed dysregulation in the same direction with greater or less than 1  $\log_2$  fold change in common in OSCC versus control between the RDH-NGS and TCGA-NGS datasets.

### Selecting miRNA for study in oral swirl RNA

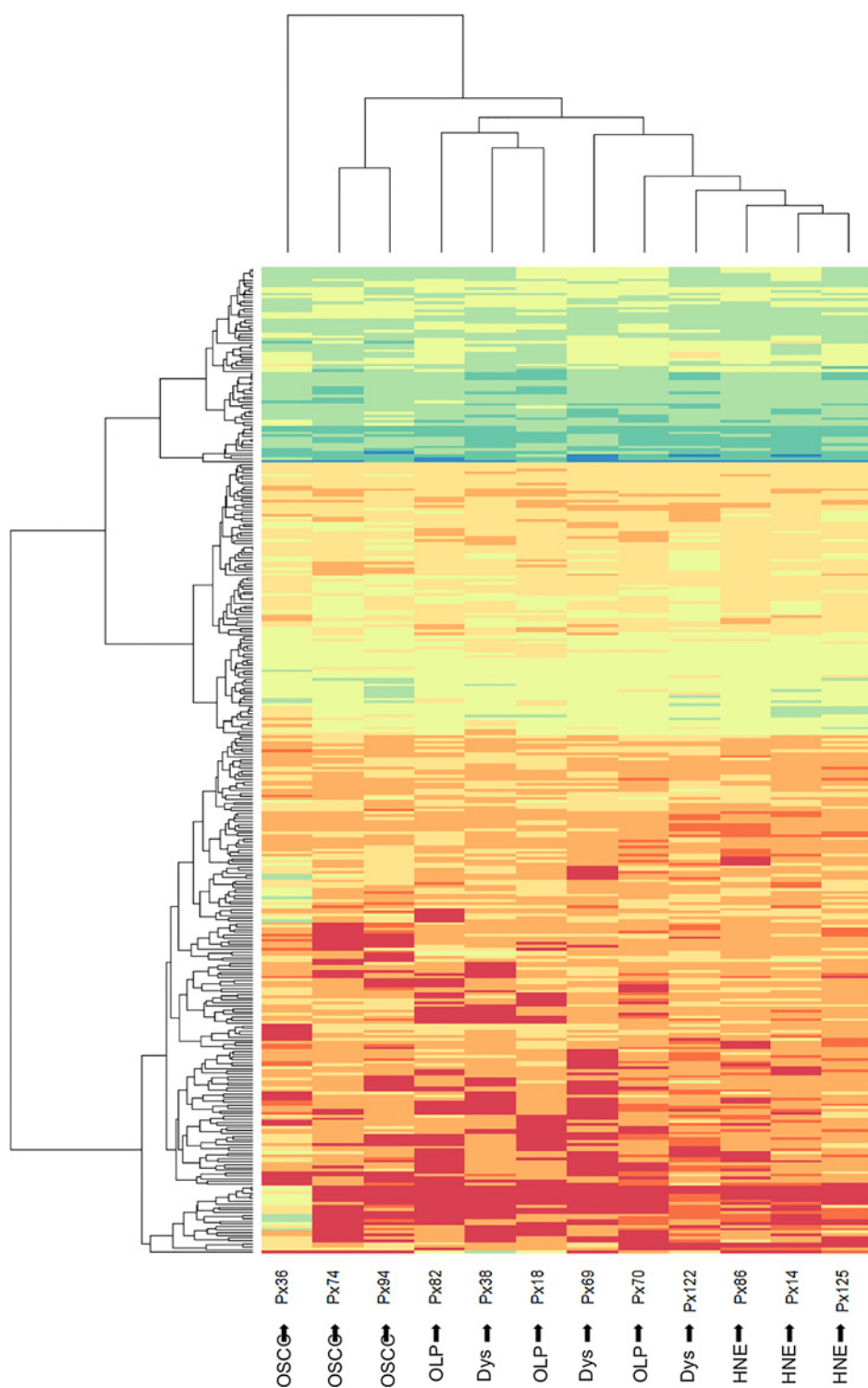
Due to the yield limit of RNA obtained in the oral swirl extracts, NGS was not feasible; hence, oral swirl extracts were analyzed by qPCR. Preliminary qPCR testing suggested that lower-abundance miRNAs were unlikely to be consistently detected; therefore, miRNAs with abundance levels less than the mean read count of both datasets were not examined. A panel of 6 miRNAs of interest remained from the 29 in-common miRNAs: miR-31-5p, miR-21-5p, miR-125b-5p, miR-99a-5p, miR-100-5p, and let-7c-5p (Table 1). The miRNAs identified were also found to be dysregulated in OSCC relative to OLP and OSCC relative to dysplasia (Fig. 2C). In addition to the six dysregulated miRNAs, two normalization miRNAs were selected, which displayed little variation across RDH-NGS and TCGA-NGS datasets. MiRNA miR-24-3p was consistently abundant, was within the top 5 least variable miRNAs, and has been shown to be highly abundant in saliva and oral swirls (6, 14). miR-30c was the least variable miRNA with mid-range abundance across all disease states in the RDH-NGS data.

### Analyzing miRNA dysregulation in oral swirl RNA training set

The 8 miRNAs were studied in a training set of 15 OSCC-OS samples and 15 C-OS samples. It was found that miR-31-5p was undetectable in both the OS samples tested and a human heart RNA control. However, miR-31-5p was detected in an OSCC FFPE sample [patient P-74 (SCC)] using RT-qPCR, suggesting that miR-31-5p expression in OS is low and was therefore excluded from further analysis. The other seven studied miRNAs were consistently detected in both OSCC-OS and C-OS samples tested in all but two single miRNA assays. Where expression was undetermined, a  $C_t$  value was replaced by numerical value of 40.

To test if our selected normalizers (miR-24-3p and miR-30c-5p) were suitable for comparisons with the other miRNA, we systematically used each quantified miRNA as a normalizer and examined the effect of this on the abundance distribution for all other miRNAs. Difference in  $C_t$  from the candidate normalizer was

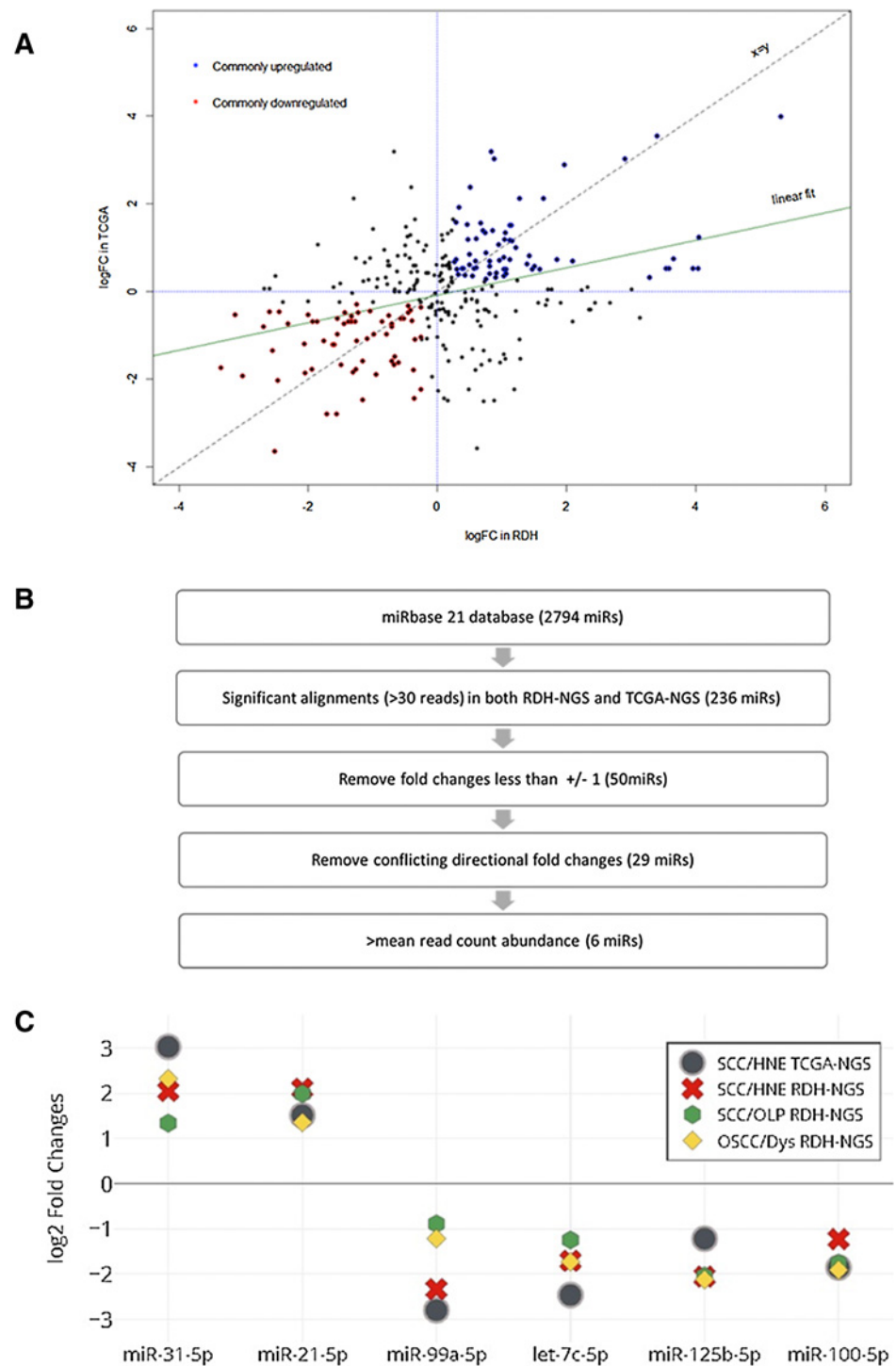
Yap et al.



**Figure 1.** RDH-NGS dendrogram of hierarchical clustering of miRNA >30 reads per million—heat map shows clustering of OSCC and HNE samples on either ends of the spectrum with OLP and dysplasia (Dys) samples alternating in between.

calculated. miR30-c-5p was suitable as a normalizer, but the greatest difference between C-OS and OSCC-OS was found by using miR-99a alone, and subsequent analysis was made using this miRNA (Fig. 4A). It was found that

miR-24-3p was significantly different in abundance (unpaired *t* test,  $P = 0.037$ ) between OSCC-OS and C-OS sample RNA and not suitable as a reference miRNA; however, it was included in all subsequent analyses due

**Figure 2.**

**A**, Scatterplot of  $\log_2$  fold changes of OSCC over HNE for the RDH-NGS versus TCGA-NGS datasets; commonly upregulated miRNAs are indicated in blue, whereas commonly downregulated miRNAs are indicated in red. **B**, Flow chart of selection of miRNAs from the miRbase database for analysis. **C**,  $\log_2$  fold changes of the panel of 6 dysregulated miRNAs between OSCC and HNE using both the RDH-NGS and TCGA-NGS data and OSCC versus OLP and OSCC versus dysplasia with the RDH-NGS.

to this dysregulation. MiR-21, let-7c, and miR-100 abundances were found to be significantly different between OSCC-OS and C-OS (Fig. 4A).

A "dysregulation score" was developed to display the cumulative significant dysregulation of the studied miRNA. The difference in  $C_t$  of miR-24-3p, miR-21-5p,

let-7c-5p, and miR-100-5p from the  $C_t$  of miR-99-5p of each sample from the C-OS mean was summed. The resultant number was designated the sample's dysregulation score. Comparing the dysregulation score of the first 15 OSCC-OS versus 15 C-OS yielded an AUC of 0.95 [95% confidence interval (CI), 0.88–1.03; Fig. 4B and C].

Yap et al.

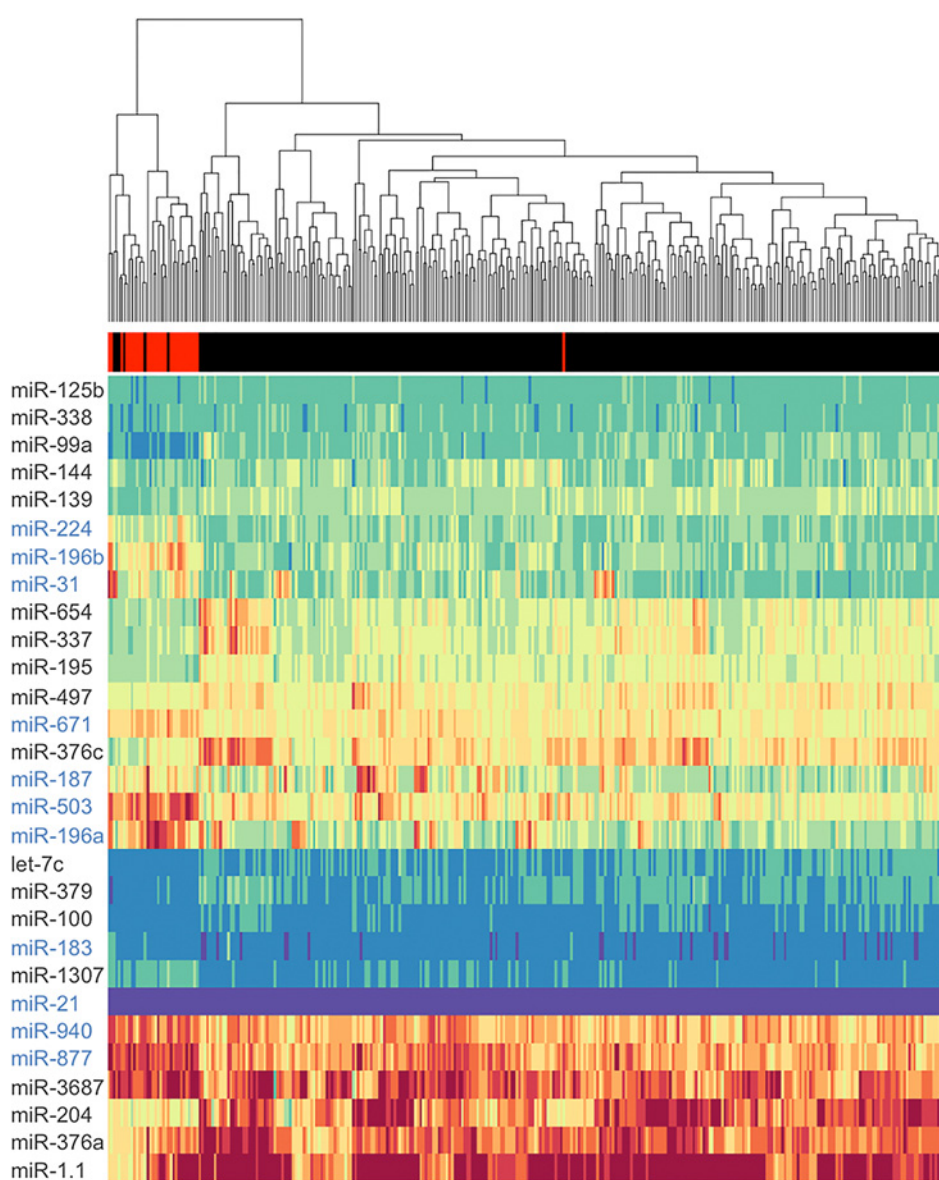


**Figure 3.** Hierarchical cluster analysis of TCGA-NGS and the 29 miRNAs with fold changes greater (*blue*) or less (*gray*) than 1 ( $\log_2$ ) in common with the RDH-NGS. OSCC ( $n = 292$ ) are displayed in *black* versus normal ( $n = 39$ ) in *red*.

### Test cohort

A further test cohort of 15 OSCC-OS versus 15 C-OS samples was analyzed as above and yielded a AUC of 0.86 (95% CI, 0.79–1.00; Fig. 4B and C).

### Development of classification tree algorithm for high-accuracy identification of OSCC-OS

A classification tree was used to create an algorithm based upon the significantly dysregulated miRNAs miR-21, let-7c, and miR-100 in combination with the dysregulation score, dividing the subjects into "LOW" and "HIGH" likelihood of presence of OSCC. The order and cutoff for each miRNA were selected to allow for 100% sensitivity of OSCC-OS as "HIGH" and the highest identification of C-OS as "LOW" likelihood (Fig. 5).

The conditions of the classification tree were as follows: IF let-7-5p ( $<-1.00$ , "HIGH") ( $>3.38$ , "LOW") otherwise ("RISK")

IF miR-21-5p ( $>3.22$ , "HIGH") ( $<0.745$ , "LOW") otherwise ("RISK")

IF miR-100-5p ( $<-6.98$ , "HIGH") ( $>2.90$ , "LOW") otherwise ("RISK")

IF Dysregulation Score ( $<7.15$ , "LOW") otherwise "HIGH"

Utilizing this classification tree, all (30/30) of OSCC could be identified as "HIGH" likelihood, and 70% (21/30) of C-OS identified as "LOW" likelihood.

Overall, our results show a panel of miRNA were consistently detected in oral swirls and displayed dysregulation that could be used to correctly identify OSCC-OS and C-OS with high accuracy.

**Table 1.** Dysregulation of miRNAs studied in the literature, RDH-NGS versus TCGA-NGS, and oral swirls

miRNA	Location	Role in oral cancer	Dysregulation in oral cancer	Common dysregulation in RDH-NGS vs. TCGA OSCC/HNE	Findings in oral swirls (OSCC-OS/C-OS) normalized to miR-99a-5p
miR-31	9p21.3	Oncogenic (30, 31)	Upregulated in OSCC tissues (15), plasma (32), cell lines (33), murine model (28)	miR-31-5p Upregulated	-
miR-21	17q23.1	Oncogenic (34, 35)	Upregulated in OSCC tissues (36–38), cell lines (34), serum (27, 39, 40)	miR-21-5p Upregulated	miR-21-5p Upregulated
miR-99a	21q21.1	Tumor suppressor (41–43)	Downregulated in OSCC tissues (42–44)	miR-99a-5p Downregulated	miR-99a-5p Used as reference
let-7c	21q21.1	Not reported	Downregulated in OSCC tissues (44)	let-7c-5p Downregulated	let-7c-5p Downregulated
miR-125b	11q24.1 21q21.1	Tumor-suppressive (45) and radiosensitizing (46)	Downregulated in OSCC cell lines and tumors (19) (40, 44)	miR-125b-5p Downregulated	miR-125b-5p No significant difference to miR-99a-5p
miR-100	11q24.1	Tumor suppressive (20)	Downregulated in OSCC cell lines and tumors (44, 47)	miR-100-5p Downregulated	miR-100-5p Downregulated
miR-24	9q22.32 19p13.12	Oncogenic (48, 49)	Upregulated in cell lines (49), tissue, and serum (50)	miR-24-3p Low variation	miR-24-3p Upregulated
miR-30c	1p34.2 6q13	Not reported	Not reported	miR-30c-5p Low variation	miR-30c-5p No significant difference to miR-99a-5p

## Discussion

This study, for the first time, demonstrates the clinical application of oral swirls as a source of assessable miRNA using a PEG-based extracellular vesicle enrichment method with subsequent RNA extraction and a two-step qPCR. We have clearly demonstrated that the presence of OSCC can be identified through detecting dysregulation of cancer-associated miRNAs in oral swirls. In this study, we performed NGS on miRNA extracted from FFPE biopsy specimens and compared this with data from the TCGA database of miRNA extracted from fresh-frozen specimens comparing OSCC and controls. This enabled us to identify miRNAs that were abundant and commonly dysregulated between the two tissues types, defining 6 miRNAs to use to assess abundance in oral swirls. Yield of miRNA from formalin-fixed incisional biopsy specimens was sufficient for NGS using the workflow above.

The clinical convenience and facility afforded by utilizing oral swirls is balanced against its limited RNA yield. In the future, with technological advancement, it may be possible to obtain a comprehensive analysis of miRNA in oral swirl extracts which could lead to refining the miRNA panel developed here. Exploring the use of new sample types requires the comparison with established sample types, and although the best available comparison may be sought, the data are not necessarily translatable. In our study, this was evidenced by the variance observed in miR-24-3p abundance in oral swirl RNA extracts, whereas the abundance of this miRNA was equivalent in the OSCC versus HNE NGS data. It is also demonstrated in the difficulty in detecting miR-31-5p in oral swirl extracts and heart RNA, yet it was an abundant miRNA in the FFPE and fresh-frozen resection tissue NGS data and previously detected by others in saliva (15).

A panel of miRNAs that were commonly dysregulated in OSCC versus control FFPE samples and fresh-frozen samples was successfully identified and appeared suitable for study in oral swirls. All identified miRNAs were reported as dysregulated in oral cancer from heterogeneous studies in the literature and no reports of conflicting directional dysregulation (Table 1). This dysregulation may represent a common signature of transcriptome aberration in oral cancer across tissues types and could be useful for early identification of OSCC. Further, it was important that this signature was also demonstrated in OSCC versus OLP and OSCC versus dysplasia in the RDH-NGS data, highlighting its potential for use in predicting malignant transformation in these common potentially malignant oral mucosal disorders.

Although the selection method considered each miRNA individually and independently, it was interesting to discover that the downregulated miRNAs (miR-99a, let-7c, miR-125b, and miR-100) were part of two miR-99a/100–125b clusters encoded on human chromosomes 11 and 21 (16). miR-99a, let-7c, and 125b have been found to be downregulated as a cluster in prostate cancer (17) and cholangiocarcinoma (18). miR-125b and miR-100 have previously been found to be downregulated together in laser-dissected cells from OSCC tumors and cell lines (19) and supported to target the IGF1R–Akt–mTOR pathway in head and neck SCC (20).

Salivary miRNAs have been increasingly explored in the diagnosis of cancer over the last decade (14), including in head and neck cancer (21), and specifically for patients with salivary gland neoplasms (22), esophageal cancer (23), and OSCC (7). Protocols have included stimulated or unstimulated saliva for analysis of either whole saliva or salivary supernatant. Majority of miRNAs detectable in saliva are reported to be concentrated in extracellular

Yap et al.

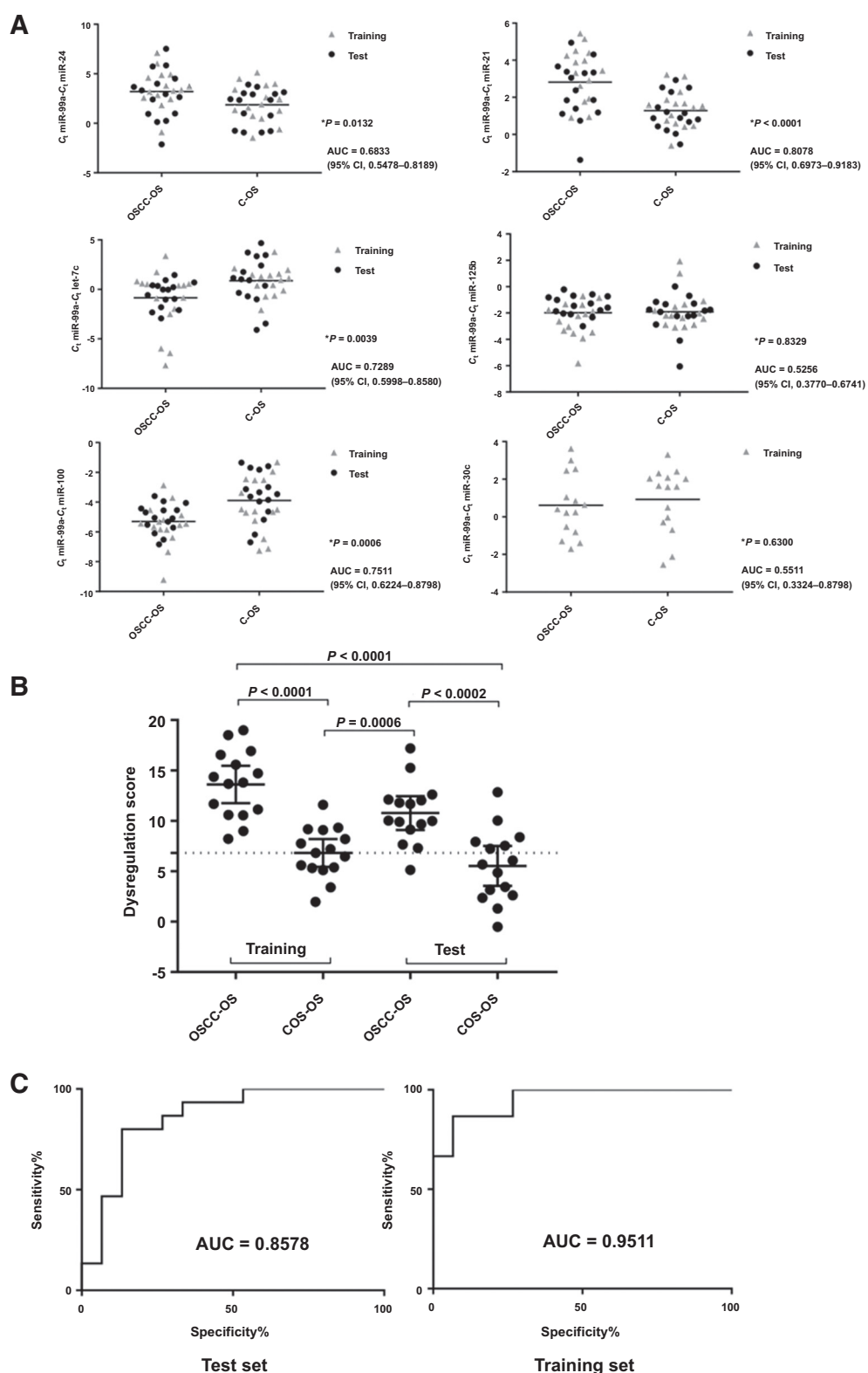


**Figure 4.** **A**, Difference in C<sub>t</sub> of training and test sets OSCC-OS versus C-OS samples for miR-24-3p, miR-21-5p, let-7c-5p, miR-125b-5p, miR-100-5p, and miR-30c-5p from miR-99a-5p with *t* test *P* value and AUC. **B**, Dysregulation score plot of training and test cohorts of OSCC-OS versus COS-OS. **C**, ROC curve of the dysregulation score for training and test cohorts of OSCC-OS versus COS-OS.

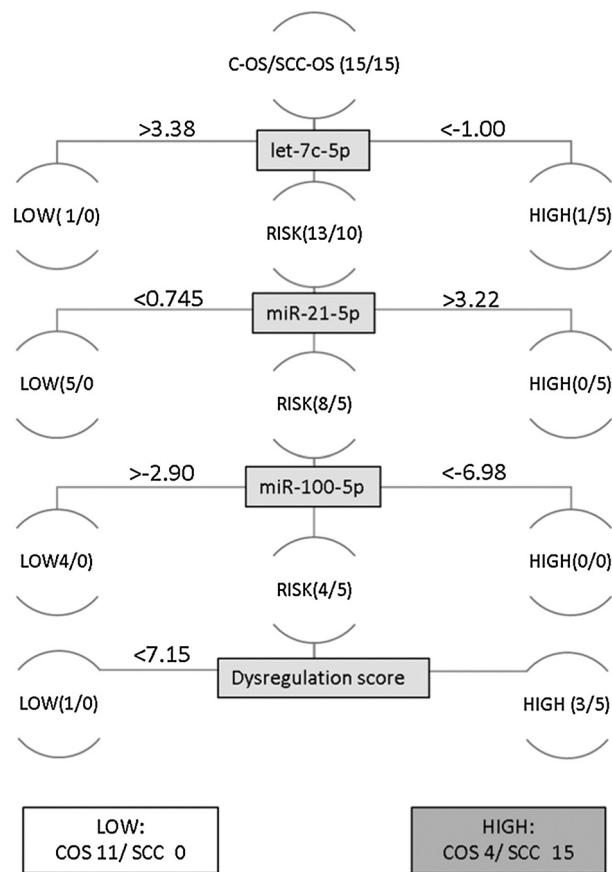


**Figure 5.**

Classification tree dividing samples into HIGH or LOW likelihood of presence of OSCC using 4 tiers. All (15/15) OSCC-OS are identified as HIGH likelihood, and 11/15 (73.3%) of C-OS are identified as LOW likelihood.

vesicles, primarily exosomes (24). OSCC cells that have sourced miR-21-rich exosomes have been shown to promote prometastatic behavior in neighboring cells (25), and the other miRNAs in our panel have not previously been studied in OSCC-associated exosomes. Variable salivary miRNAs have been highlighted of interest in OSCC. Candidates in common with our study include overexpression of miR-21 (15, 26), miR-31, and miR-24 (7). A recent meta-analysis showed that circulating miR-21 may be a potential biomarker as a diagnostic tool for early-stage cancer diagnosis of various carcinomas, and salivary miR-21 has been found to be upregulated in esophageal, colorectal, and pancreatic cancer patients (27). It may be that upregulation of miR-21 in oral swirls represents a sensitive but less specific indicator of malignancy, not just OSCC. In a murine model, progressive increase of miR-21 and miR-31 was noted in saliva with 4NQO-induced epithelial pathogenesis (28). miR-31 has also been of interest in saliva of OSCC and OPMD patients, although its detection in human OPMD has featured conflicting results (29). Although miR-31 was not detectable in oral

swirls, it remains an miRNA of interest in the study of OSCC development, although miRNAs which can clearly differentiate OSCC versus OPMD likely provide greater clinical utility than those which distinguish between controls versus OSCC and OPMD together. To date, significant dysregulation of miR-99a, let-7c, miR-125b, and miR-100 has not previously been highlighted in saliva. Further, no studies have investigated dysregulation of miRNAs in oral swirls.

Oral swirl collection could be administered or prescribed by a medical or dental practitioner in a primary care setting or as an adjunctive tool to longitudinal follow-up of an OPMD in specialist care. Using the workflow as outlined in the present study, the time from receipt or defrost of a sample to qPCR result could occur in less than 24 hours. Further samples are of course necessary to increase the power of the test, and parameters of the algorithm may become further adjusted to ensure sensitivity. The developed algorithm provides a strong foundation from which further samples can be analyzed and used to interrogate the robustness of the test. Future samples could be added to the test development to decrease the standard deviation observed for the clinically normal oral swirl samples. It is not expected that absolutely all OSCCs will exhibit identical dysregulation, outliers will undoubtedly be encountered, and the frequency of such outliers needs to be elucidated. It may be more appropriate to create an intermediate tiered RISK category to identify borderline scores in the decision tree and provide a safety net for these expected outliers. Nevertheless, the present study provides proof of concept that oral swirls may present a suitable sample type to detect the presence of disease-associated miRNAs, including in malignancy.

## Conclusion

We present a promising avenue for detection of miRNAs in oral swirls as an adjunctive stratification tool for disease states, here demonstrated for OSCC. This is the first time that detection and dysregulation of cancer-associated miRNAs have been demonstrated in oral swirls. Further studies to validate these findings in OSCC and other oral mucosal disease conditions are warranted.

## Disclosure of Potential Conflicts of Interest

No potential conflicts of interest were disclosed.

## Authors' Contributions

**Conception and design:** T. Yap, E. Reynolds, C. Seers, M. McCullough  
**Development of methodology:** T. Yap, K. Koo, L.J. Vella, C. Seers, M. McCullough

**Acquisition of data (provided animals, acquired and managed patients, provided facilities, etc.):** T. Yap, A. Natri

**Analysis and interpretation of data (e.g., statistical analysis, biostatistics, computational analysis):** T. Yap, K. Koo, L. Cheng, A.F. Hill, M. McCullough

Yap et al.

**Writing, review, and/or revision of the manuscript:** T. Yap, K. Koo, L.J. Vella, A.F. Hill, E. Reynolds, N. Cirillo, C. Seers, M. McCullough  
**Administrative, technical, or material support (i.e., reporting or organizing data, constructing databases):** T. Yap, E. Reynolds, A. Nastri, M. McCullough

**Study supervision:** A. Nastri, N. Cirillo, C. Seers, M. McCullough

## Acknowledgments

The results shown here are in part based upon data generated by the TCGA Research Network: <http://cancergenome.nih.gov/>. This work was supported by the Australian Dental Research Foundation (ADRF), the Australia and New Zealand Head and Neck Cancer

Society Research Foundation (ANZHNSRF), National Health and Medical Research Council (NHMRC)-Postgraduate Scholarship, and Australian Government Research Training Program (AGRTP) Scholarship.

The costs of publication of this article were defrayed in part by the payment of page charges. This article must therefore be hereby marked *advertisement* in accordance with 18 U.S.C. Section 1734 solely to indicate this fact.

Received December 14, 2017; revised March 2, 2018; accepted May 1, 2018; published first May 15, 2018.

## References

- Warnakulasuriya S, Kovacevic T, Madden P, Coupland VH, Sperandio M, Odell E, et al. Factors predicting malignant transformation in oral potentially malignant disorders among patients accrued over a 10-year period in South East England. *J Oral Pathol Med* 2011;40:677–83.
- Aghbari SMH, Abushouk AI, Attia A, Elmaraezy A, Menshaw A, Ahmed MS, et al. Malignant transformation of oral lichen planus and oral lichenoid lesions: A meta-analysis of 20095 patient data. *Oral Oncol* 2017;68:92–102.
- Scully C. Challenges in predicting which oral mucosal potentially malignant disease will progress to neoplasia. *Oral Dis* 2014;20:1–5.
- Crossman T, Warburton F, Richards MA, Smith H, Ramirez A, Forbes LJ. Role of general practice in the diagnosis of oral cancer. *Br J Oral Maxillofac Surg* 2016;54:208–12.
- Seoane-Romero JM, Vazquez-Mahia I, Seoane J, Varela-Centelles P, Tomas I, Lopez-Cedrun JL. Factors related to late stage diagnosis of oral squamous cell carcinoma. *Med Oral Patol Oral Cir Bucal* 2012;17:e35–40.
- Yap T, Vella LJ, Seers C, Nastri A, Reynolds E, Cirillo N, et al. Oral swirl samples - a robust source of microRNA protected by extracellular vesicles. *Oral Dis* 2017;23:312–7.
- Momen-Heravi F, Trachtenberg AJ, Kuo WP, Cheng YS. Genome-wide study of salivary microRNAs for detection of oral cancer. *J Dent Res* 2014;93:865–93s.
- Troiano G, Boldrup L, Ardito F, Gu X, Lo Muzio L, Nylander K. Circulating miRNAs from blood, plasma or serum as promising clinical biomarkers in oral squamous cell carcinoma: a systematic review of current findings. *Oral Oncol* 2016;63:30–7.
- Hedegaard J, Thorsen K, Lund MK, Hein AM, Hamilton-Dutoit SJ, Vang S, et al. Next-generation sequencing of RNA and DNA isolated from paired fresh-frozen and formalin-fixed paraffin-embedded samples of human cancer and normal tissue. *PLoS One* 2014;9:e98187.
- Robinson MD, McCarthy DJ, Smyth GK. edgeR: a Bioconductor package for differential expression analysis of digital gene expression data. *Bioinformatics* 2010;26:139–40.
- Wan G, Lim QE, Too HP. High-performance quantification of mature microRNAs by real-time RT-PCR using deoxyuridine-incorporated oligonucleotides and hemi-nested primers. *RNA* 2010;16:1436–45.
- Liu W, Saint DA. Validation of a quantitative method for real time PCR kinetics. *Biochem Biophys Res Commun* 2002;294:347–53.
- Vandesompele J, De Preter K, Pattyn F, Poppe B, Van Roy N, De Paepe A, et al. Accurate normalization of real-time quantitative RT-PCR data by geometric averaging of multiple internal control genes. *Genome Biol* 2002;3:research0034.1.
- Park NJ, Zhou H, Elashoff D, Henson BS, Kastratovic DA, Abemayor E, et al. Salivary microRNA: discovery, characterization, and clinical utility for oral cancer detection. *Clin Cancer Res* 2009;15:5473–7.
- Hung KF, Liu CJ, Chiu PC, Lin JS, Chang KW, Shih WY, et al. MicroRNA-31 upregulation predicts increased risk of progression of oral potentially malignant disorder. *Oral Oncol* 2016;53:42–7.
- Emmrich S, Rasche M, Schoning J, Reimer C, Keihani S, Maroz A, et al. miR-99a/100~125b tricistrons regulate hematopoietic stem and progenitor cell homeostasis by shifting the balance between TGFβ and Wnt signaling. *Genes Dev* 2014;28:858–74.
- Sun D, Layer R, Mueller AC, Cichewicz MA, Negishi M, Paschal BM, et al. Regulation of several androgen-induced genes through the repression of the miR-99a/let-7c/miR-125b-2 miRNA cluster in prostate cancer cells. *Oncogene* 2014;33:1448–57.
- Lin KY, Ye H, Han BW, Wang WT, Wei PP, He B, et al. Genome-wide screen identified let-7c/miR-99a/miR-125b regulating tumor progression and stem-like properties in cholangiocarcinoma. *Oncogene* 2016;35:3376–86.
- Wong TS, Liu XB, Wong BY, Ng RW, Yuen AP, Wei WI. Mature miR-184 as potential oncogenic microRNA of squamous cell carcinoma of tongue. *Clin Cancer Res* 2008;14:2588–92.
- Chen Z, Jin Y, Yu D, Wang A, Mahjabeen I, Wang C, et al. Down-regulation of the microRNA-99 family members in head and neck squamous cell carcinoma. *Oral Oncol* 2012;48:686–91.
- Greither T, Vorwerk F, Kappler M, Bache M, Taubert H, Kuhnt T, et al. Salivary miR-93 and miR-200a as post-radiotherapy biomarkers in head and neck squamous cell carcinoma. *Oncol Rep* 2017;38:1268–75.
- Matse JH, Yoshizawa J, Wang X, Elashoff D, Bolscher JG, Veerman EC, et al. Human salivary micro-RNA in patients with parotid salivary gland neoplasms. *PLoS One* 2015;10:e0142264.
- Xie Z, Chen G, Zhang X, Li D, Huang J, Yang C, et al. Salivary microRNAs as promising biomarkers for detection of esophageal cancer. *PLoS One* 2013;8:e57502.
- Gallo A, Tandon M, Alevizos I, Illei GG. The majority of microRNAs detectable in serum and saliva is concentrated in exosomes. *PLoS One* 2012;7:e30679.
- Li L, Li C, Wang S, Wang Z, Jiang J, Wang W, et al. Exosomes derived from hypoxic oral squamous cell carcinoma cells deliver miR-21 to normoxic cells to elicit a prometastatic phenotype. *Cancer Res* 2016;76:1770–80.
- Zahran F, Ghalwash D, Shaker O, Al-Johani K, Scully C. Salivary microRNAs in oral cancer. *Oral Dis* 2015;21:739–47.
- Wu K, Li L, Li S. Circulating microRNA-21 as a biomarker for the detection of various carcinomas: an updated meta-analysis based on 36 studies. *Tumor Biol* 2015;36:1973–81.

28. Kao YY, Tu HF, Kao SY, Chang KW, Lin SC. The increase of oncogenic miRNA expression in tongue carcinogenesis of a mouse model. *Oral Oncol* 2015;51:1103–12.
29. Liu CJ, Lin SC, Yang CC, Cheng HW, Chang KW. Exploiting salivary miR-31 as a clinical biomarker of oral squamous cell carcinoma. *Head Neck* 2012;34:219–24.
30. Lu WC, Liu CJ, Tu HF, Chung YT, Yang CC, Kao SY, et al. miR-31 targets ARID1A and enhances the oncogenicity and stemness of head and neck squamous cell carcinoma. *Oncotarget* 2016;7:57254–67.
31. Kao SY, Tsai MM, Wu CH, Chen JJ, Tseng SH, Lin SC, et al. Co-targeting of multiple microRNAs on factor-Inhibiting hypoxia-Inducible factor gene for the pathogenesis of head and neck carcinomas. *Head Neck* 2016;38:522–8.
32. Liu CJ, Kao SY, Tu HF, Tsai MM, Chang KW, Lin SC. Increase of microRNA miR-31 level in plasma could be a potential marker of oral cancer. *Oral Dis* 2010;16:360–4.
33. Lu WC, Kao SY, Yang CC, Tu HF, Wu CH, Chang KW, et al. EGF up-regulates miR-31 through the C/EBP $\beta$  signal cascade in oral carcinoma. *PLoS One* 2014;9:e108049.
34. Wang Y, Zhu Y, Lv P, Li L. The role of miR-21 in proliferation and invasion capacity of human tongue squamous cell carcinoma in vitro. *Int J Clin Exp Pathol* 2015;8:4555–63.
35. Kawakita A, Yanamoto S, Yamada S, Naruse T, Takahashi H, Kawasaki G, et al. MicroRNA-21 promotes oral cancer invasion via the Wnt/ $\beta$ -catenin pathway by targeting DKK2. *Pathol Oncol Res* 2014;20:253–61.
36. Li J, Huang H, Sun L, Yang M, Pan C, Chen W, et al. MiR-21 indicates poor prognosis in tongue squamous cell carcinomas as an apoptosis inhibitor. *Clin Cancer Res* 2009;15:3998–4008.
37. Scapoli L, Palmieri A, Lo Muzio L, Pezzetti F, Rubini C, Girardi A, et al. MicroRNA expression profiling of oral carcinoma identifies new markers of tumor progression. *Int J Immunopathol Pharmacol* 2010;23:1229–34.
38. Hedback N, Jensen DH, Specht L, Fiehn AM, Therkildsen MH, Friis-Hansen L, et al. MiR-21 expression in the tumor stroma of oral squamous cell carcinoma: an independent biomarker of disease free survival. *PLoS One* 2014;9:e95193.
39. Ren W, Qiang C, Gao L, Li SM, Zhang LM, Wang XL, et al. Circulating microRNA-21 (MIR-21) and phosphatase and tensin homolog (PTEN) are promising novel biomarkers for detection of oral squamous cell carcinoma. *Biomarkers* 2014;19:590–6.
40. Yu T, Wang XY, Gong RG, Li A, Yang S, Cao YT, et al. The expression profile of microRNAs in a model of 7,12-dimethylbenz[a]anthracene-induced oral carcinogenesis in Syrian hamster. *J Exp Clin Cancer* 2009;28:64.
41. Yen YC, Shiah SG, Chu HC, Hsu YM, Hsiao JR, Chang JY, et al. Reciprocal regulation of microRNA-99a and insulin-like growth factor I receptor signaling in oral squamous cell carcinoma cells. *Mol Cancer* 2014;13:6.
42. Yan B, Fu Q, Lai L, Tao X, Fei Y, Shen J, et al. Downregulation of microRNA 99a in oral squamous cell carcinomas contributes to the growth and survival of oral cancer cells. *Mol Med Rep* 2012;6:675–81.
43. Kuo YZ, Tai YH, Lo HI, Chen YL, Cheng HC, Fang WY, et al. MiR-99a exerts anti-metastasis through inhibiting myotubularin-related protein 3 expression in oral cancer. *Oral Dis* 2014;20:e65–75.
44. Setién-Olarrá A, Bediaga NG, Acha-Sagredo A, Marichalar-Mendia X, de Pancorbo MM, Aguirre-Urizar JM. Genomewide miRNA profiling of oral lichenoid disorders and oral squamous cell carcinoma. *Oral Dis* 2016;22:754–60.
45. Nakanishi H, Taccioli C, Palatini J, Fernandez-Cymering C, Cui R, Kim T, et al. Loss of miR-125b-1 contributes to head and neck cancer development by dysregulating TACSTD2 and MAPK pathway. *Oncogene* 2014;33:702–12.
46. Shiiba M, Shinozuka K, Saito K, Fushimi K, Kasamatsu A, Ogawara K, et al. MicroRNA-125b regulates proliferation and radioresistance of oral squamous cell carcinoma. *Br J Cancer* 2013;108:1817–21.
47. Henson BJ, Bhattacharjee S, O'Dee DM, Feingold E, Gollin SM. Decreased expression of miR-125b and miR-100 in oral cancer cells contributes to malignancy. *Genes ChromosomCancer* 2009;48:569–82.
48. Zhao J, Hu C, Chi J, Li J, Peng C, Yun X, et al. miR-24 promotes the proliferation, migration and invasion in human tongue squamous cell carcinoma by targeting FBXW7. *Onc Rep* 2016;36:1143–9.
49. Liu X, Wang A, Heidbreder CE, Jiang L, Yu J, Kolokythas A, et al. MicroRNA-24 targeting RNA-binding protein DND1 in tongue squamous cell carcinoma. *FEBS Lett* 2010;584:4115–20.
50. Lin SC, Liu CJ, Lin JA, Chiang WF, Hung PS, Chang KW. miR-24 up-regulation in oral carcinoma: positive association from clinical and in vitro analysis. *Oral Oncol* 2010;46:204–8.



# Cancer Prevention Research

## Predicting the Presence of Oral Squamous Cell Carcinoma Using Commonly Dysregulated MicroRNA in Oral Swirls

Tami Yap, Kendrick Koo, Lesley Cheng, et al.

*Cancer Prev Res* 2018;11:491-502. Published OnlineFirst May 15, 2018.

**Updated version** Access the most recent version of this article at:  
doi:[10.1158/1940-6207.CAPR-17-0409](https://doi.org/10.1158/1940-6207.CAPR-17-0409)

**Cited articles** This article cites 49 articles, 6 of which you can access for free at:  
<http://cancerpreventionresearch.aacrjournals.org/content/11/8/491.full#ref-list-1>

**E-mail alerts** [Sign up to receive free email-alerts](#) related to this article or journal.

**Reprints and Subscriptions** To order reprints of this article or to subscribe to the journal, contact the AACR Publications Department at [pubs@aacr.org](mailto:pubs@aacr.org).

**Permissions** To request permission to re-use all or part of this article, use this link <http://cancerpreventionresearch.aacrjournals.org/content/11/8/491>.  
Click on "Request Permissions" which will take you to the Copyright Clearance Center's (CCC) Rightslink site.